

# Development of a Bacterial Biosensor for Rapid Screening of Yeast *p*-Coumaric Acid Production

Solvej Siedler,<sup>†</sup> Narendar K. Khatri,<sup>†,‡</sup> Andrea Zsohár,<sup>†</sup> Inge Kjærbølling,<sup>†</sup> Michael Vogt,<sup>§</sup> Petter Hammar,<sup>‡</sup> Christian F. Nielsen,<sup>†</sup> Jan Marienhagen,<sup>§</sup> Morten O. A. Sommer,<sup>\*,†</sup> and Haakan N. Joensuu<sup>†,‡</sup>

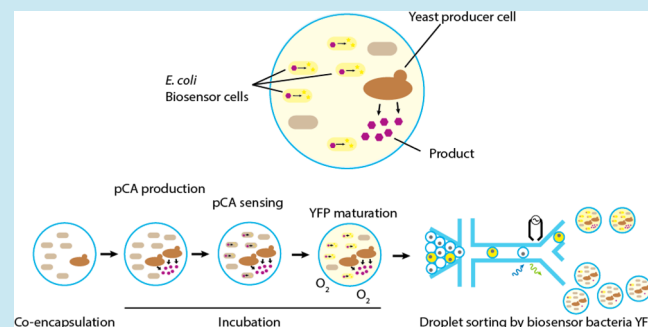
<sup>†</sup>Novo Nordisk Foundation Center for Biosustainability, Technical University of Denmark, Kogle Alle 6, Hørsholm, 2970, Denmark

<sup>‡</sup>Division of Proteomics and Nanobiotechnology, Science for Life Laboratory, KTH Royal Institute of Technology, Stockholm, 114 28, Sweden

<sup>§</sup>Institute of Bio- and Geosciences IBG-1: Biotechnology, Forschungszentrum Jülich GmbH, Jülich, 52425, Germany

## Supporting Information

**ABSTRACT:** Transcription factor-based biosensors are used to identify producer strains, a critical bottleneck in cell factory engineering. Here, we address two challenges with this methodology: transplantation of heterologous transcriptional regulators into new hosts to generate functional biosensors and biosensing of the extracellular product concentration that accurately reflects the effective cell factory production capacity. We describe the effects of different translation initiation rates on the dynamic range of a *p*-coumaric acid biosensor based on the *Bacillus subtilis* transcriptional repressor PadR by varying its ribosomal binding site. Furthermore, we demonstrate the functionality of this *p*-coumaric acid biosensor in *Escherichia coli* and *Corynebacterium glutamicum*. Finally, we encapsulate yeast *p*-coumaric acid-producing cells with *E. coli*-biosensing cells in picoliter droplets and, in a microfluidic device, rapidly sort droplets containing yeast cells producing high amounts of extracellular *p*-coumaric acid using the fluorescent *E. coli* biosensor signal. As additional biosensors become available, such approaches will find broad applications for screening of an extracellular product.



While genome engineering techniques have undergone a revolution over the past decade, screening for high-producing cells and identifying the best enzymes involved in biocatalysis remain major bottlenecks in cell factory engineering. Genome engineering techniques have enabled the rapid generation of libraries consisting of thousands, and even millions, of cell factory mutants, each potentially carrying beneficial mutations.<sup>1–3</sup> Transcription factor-based biosensors are well suited for high-throughput screening approaches. These biosensors couple the intracellular concentration of small molecules to a detectable read-out, for example, the expression of a fluorescent protein. This process enables the identification and sorting of cells with high intracellular concentrations of a specific metabolite based on fluorescence using fluorescence-activated cell sorting (FACS).

In recent years, biosensors have been developed to measure and screen the intracellular concentrations of several small metabolites.<sup>4–7</sup> Moreover, biosensor-based screens have been combined with genome engineering techniques such as recombineering<sup>8,9</sup> and screening for NADPH-dependent enzymes by measuring the redox state of the cell.<sup>10</sup> Many of the biosensors described in the literature are based on endogenous transcription factors,<sup>5</sup> which are assumed to

possess adequate expression strength as well as to exhibit autoregulation and correct folding. If the *E. coli* genome does not encode a transcription factor that can sense the desired effector molecule, heterologous transcription factors can be suitable alternatives.<sup>7</sup> However, the sensor assemblies often need to be engineered, which limits the broader adoption of biosensors as a screening tool. Designing a robust biosensor for use in multiple hosts is still particularly challenging. Furthermore, the fact that biosensors are constrained to intracellular measurements at the single-cell level restricts their use as a screening method. Screening methods should not solely rely on intracellular concentration measurements, particularly if the intracellular concentration is low due to the overexpression of exporters.<sup>11</sup> Moreover, FACS cannot be used to isolate clones that overproduce extracellular metabolites such as lactate or xylitol because increased metabolite accumulation in a culture consisting of genetically different variants cannot be linked to the specific cells with improved production capacity.<sup>12</sup> It is therefore important to develop a screening approach that can address these problems.<sup>12</sup>

**Received:** January 9, 2017

**Published:** May 23, 2017

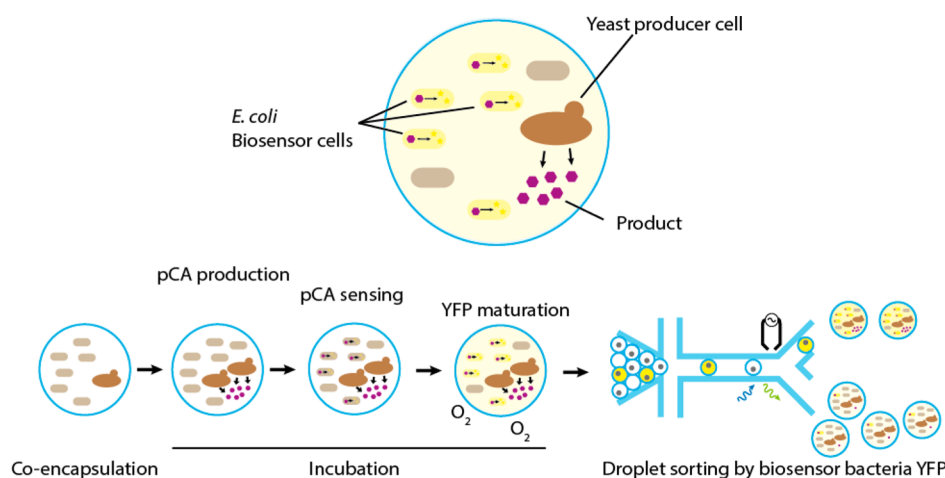


**Figure 1.** Co-encapsulated biosensors in picoliter droplets. Sensor cells (*E. coli*) and producer cells (yeast producers) are encapsulated in a picoliter droplet in a microfluidic device. Droplets are incubated at conditions favoring the production of the effector metabolite by producer cells. Extracellular *p*-coumaric acid produced by the yeast cells is captured in the droplet and induces the expression of the reporter gene (YFP) in the coencapsulated biosensor cells. Droplets are subsequently sorted in a second microfluidic device based on the fluorescence signal from the biosensor cells to enrich for productive yeast clones.

Droplet microfluidics is a technology platform wherein cells can be cultivated and processed as single cells or genetically identical microcolonies in monodisperse picoliter droplets, with each droplet functioning as a separate growth container. Droplets are rapidly and uniformly generated and processed in microfluidic devices. Encapsulation in these droplets allows the product to be retained in a picoliter volume together with the producer cell so that small amounts of an extracellular product generated by a single cell or clone can be assayed. Droplets can be further analyzed based on their fluorescence<sup>13</sup> and can be processed in multiple steps<sup>14</sup> and sorted at a throughput of millions of droplets per hour.<sup>15</sup> Droplet microfluidics has been used to screen cell variant libraries for secreted protein production<sup>16,17</sup> and secreted enzyme variants<sup>15</sup> and has been used in conjunction with enzymatic assays when the assay product is not retained in the cell.<sup>12,18</sup> With this technology, it is also possible to couple the extracellular concentration of a metabolite to a biosensor cell output by cocultivating the producer and biosensing cells in droplets (Figure 1). Coculturing an *E. coli* strain possessing biosensing functionality with a *Bacillus subtilis* production strain has been demonstrated in nanoliter-scale gel capsules.<sup>19</sup> These ~400  $\mu\text{m}$  sized-gel capsules, which encase thousands of sensor cells and a single or a few producer cells, were sorted after isolation and the washing step. Droplet microfluidics should enable more exact control of the vessel volume, eliminate the need for a gelling agent, and decrease the vessel volume, increasing throughput by orders of magnitude.

We wanted to create a robust, *p*-coumaric acid-responsive biosensor, which is functional in different hosts. *p*-Coumaric acid is an important precursor for the production of a variety of plant natural products, including flavonoids, lignans and stilbenes.<sup>20</sup> There is no known homologous transcription factor that recognizes *p*-coumaric acid in *E. coli*, but a transcriptional repressor (PadR) and the promoter it regulates are present in *Bacillus subtilis*.<sup>21,22</sup> The production of *p*-coumaric acid has been demonstrated in several organisms, such as yeast, *Lactococcus lactis*, and *E. coli*, using enzymes of different origins; yeast has proven the best host for *p*-coumaric acid production.<sup>23–25</sup> In yeast, the translational machinery is more complex and involves only a few “one-component” transcrip-

tional regulators that sense small molecules and regulate gene expression simultaneously,<sup>26</sup> thereby restricting the range of the application of homologous transcription factor-based biosensors in yeast. In this study, we demonstrate that picoliter droplet technology can be used to overcome this limitation by cocultivation of *E. coli* and yeast.

## RESULTS AND DISCUSSION

**Biosensor Design.** To create a biosensor for the detection of *p*-coumaric acid, we identified a transcriptional regulator, PadR, that is naturally responsive to *p*-coumaric acid. PadR acts as a transcriptional repressor and inhibits the expression of PadC, a phenolic acid decarboxylase. In the presence of phenolic acids, similar to *p*-coumaric acid and ferulic acid, the transcriptional regulator is inactivated and *padC* is cotranscribed with the uncharacterized upstream genes *yveFG* in *B. subtilis*. It has been shown that PadR can be functionally expressed in *E. coli*, resulting in a 30-fold increase in PadC activity after the addition of *p*-coumaric acid but with very low absolute PadC activity.<sup>22</sup> The expression of transcriptional repressors must be tightly regulated because excessive expression results in a state of constitutive repression, whereas insufficient expression does not result in the repression of the target gene, even in the absence of an inducer.<sup>27</sup> Previous results suggested that the expression level of PadR was too high in *E. coli* because the PadC promoter was always strongly repressed. We therefore decided to alter the expression level of PadR by using two ribosomal binding sites (RBSs) of different strengths, as predicted by the RBS calculator.<sup>28</sup> One sequence lacked an RBS (translation rate: 43 au), while the other exhibited 10-fold lower predicted expression strength (translation rate: 3665 au) compared to the wild-type sequence (translation rate: 38 000 au) (Figure 2). The algorithm included additional bases, forming a hairpin structure, to obtain these low translation rates. We designed the sensor to contain the *padR* promoter and PadR protein as well as the *padC* promoter to control the expression of *yveFG* and *padC* (Figure 2). To obtain a simple readout of the *padC* promoter in subsequent screening applications, we replaced the *padC* gene with the gene for a yellow fluorescent protein (YFP). We

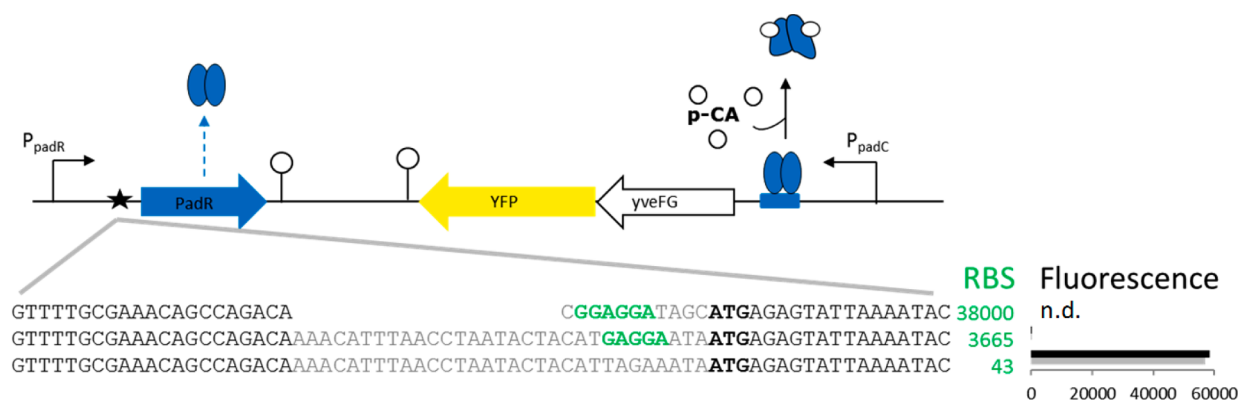


**Figure 2.** Schematic view of the PadR regulatory system. Genes, promoters, and hairpin structures that function as transcriptional terminators are indicated by thick arrows, bent arrows, and stem loops, respectively. Organization of the biosensor construct is based on the *padR* and *yveFG/ PadC* gene regions. The DNA fragment covering the natural *padR* promoter and *padR* gene, as well as a copy of the *padC* promoter controlling *yveFG* and YFP gene expression, is shown. YFP was inserted in place of the native *padC* gene. PadR (blue ovals) dimerizes and binds the PadR binding site (blue box) located in the *padC* promoter region, thereby repressing *yveFG* and YFP. PadR binding is inhibited by *p*-coumaric acid (small white circles), which leads to the derepression of the regulon members *yveFG* and YFP. The RBS and the surrounding sequence in front of *padR* were modified (star). The original sequence as well as the sequence variants are shown together with their predicted RBS strengths and measured YFP fluorescence following overnight cultivation with medium containing 1 mM *p*-coumaric acid (black) or no *p*-coumaric acid (gray). Abbreviations: n.d.: not determined; *p*-CA: *p*-coumaric acid.

analyzed the fluorescence of the resultant constructs with and without *p*-coumaric acid. The construct without a functional RBS exhibited the expected phenotype, with a high fluorescent signal produced independently of the presence of an inducer (Figure 2). This result demonstrates that the cellular concentration of PadR is insufficient to repress all *padC*/YFP promoters present in the cell. Interestingly, the variant predicted to exhibit 10 times reduced expression strength did not produce the desired phenotype; no fluorescence was detected even in the presence of an inducer (Figure 2). These data demonstrate the need to fine-tune the PadR expression level in order to construct a functional *p*-coumaric acid biosensor in *E. coli*.

**Biosensor Optimization by Random RBS Mutagenesis.** To construct a robust biosensor, we needed to determine the optimal expression strength of PadR. Because we were targeting the RBS to reduce expression strength (*i.e.*, lower than 3665 au), we mutagenized the PadR RBS and screened the resultant library for functional biosensors. We found that random mutagenesis generated many sequences that resulted in low expression strength.<sup>29</sup> We analyzed the *p*-coumaric acid response of 33 clones from this library (Figure 3a) and identified several promising candidates exhibiting a low fluorescence value in the absence of *p*-coumaric acid and a high fluorescence value in the presence of *p*-coumaric acid. The best clone exhibited 130-fold induction in the presence of the effector *p*-coumaric acid. The seven strains showing the highest fold-change upon induction were sequenced and further analyzed. Additionally, we chose two strains for use as controls: one clone harboring a constitutive “off” variant (C4) and another harboring a constitutive “on” variant (B5). The RBS calculator<sup>28</sup> predicted the theoretical RBS strength of the obtained sequences, and a narrow range of optimal RBS strengths (100–250 au) was determined (Figure 3b and Supplementary Table 2). Sequences containing an RBS with a lower predicted value resulted in a constitutive “on” state, and a higher predicted RBS strength resulted in a constitutive “off” state of the biosensor. Many natural transcriptional repressors are known, and the information presented here will help to

optimize different heterologous transcriptional repressors for optimal biosensor design.

**Characterization of the Biosensor.** We subcloned the sensor module of the construct pG-*padR*-B11, which produced the best dynamic range, into the plasmid pSEVA421 to obtain a lower copy number (4–7 copies per cell).<sup>30</sup> We analyzed the specific fluorescence of the cells containing the sensor plasmid (EcPadR) in the presence of different *p*-coumaric acid concentrations (Figure 3c and Supplementary Figure 1). A linear correlation between YFP fluorescence and *p*-coumaric acid in the range between 0.1 and 1 mM was observed. To analyze the effector range, we tested the strain EcPadR in the presence of various structurally similar compounds (Figure 3d). Of the tested chemicals, only *p*-coumaric acid acted as an inducer.

Some transcription factors involved in *p*-coumaric acid degradation have been shown to utilize *p*-coumaroyl-CoA as an effector.<sup>31,32</sup> *p*-Coumaric acid is catalyzed to *p*-coumaroyl-CoA as a first step in its degradation pathway. Because no *E. coli* gene is known to catalyze this reaction, we transformed the sensor construct into *C. glutamicum* to determine whether it reacts to *p*-coumaric acid, *p*-coumaroyl-CoA, or both. Wild-type *C. glutamicum* can convert *p*-coumaric acid into *p*-coumaroyl-CoA, whereas the  $\Delta$ *phdA* mutant does not.<sup>33</sup> We therefore subcloned the sensor module into the *C. glutamicum*-compatible plasmid pCLTON2-SC*padR*. After transformation into wild-type and  $\Delta$ *phdA* mutant *C. glutamicum* cells, the fluorescence in the presence and absence of supplemental *p*-coumaric acid was quantified (Figure 3e). The sensor was active in wild-type *C. glutamicum* cells as well as in the mutant strain, suggesting that the sensor recognizes *p*-coumaric acid. The weaker fluorescence signal in the wild-type cells compared to the  $\Delta$ *phdA* mutant can be attributed to the capacity of wild-type *C. glutamicum* to rapidly degrade *p*-coumaric acid.<sup>33</sup> Interestingly, the sensor construct optimized in *E. coli* was active without further modification in *C. glutamicum*. In *B. subtilis*, there might be another regulatory element that maintains low expression of the repressor that is not included in the sensor construct and is therefore missing in *E. coli* and *C. glutamicum*. *C. glutamicum* is an industrially important

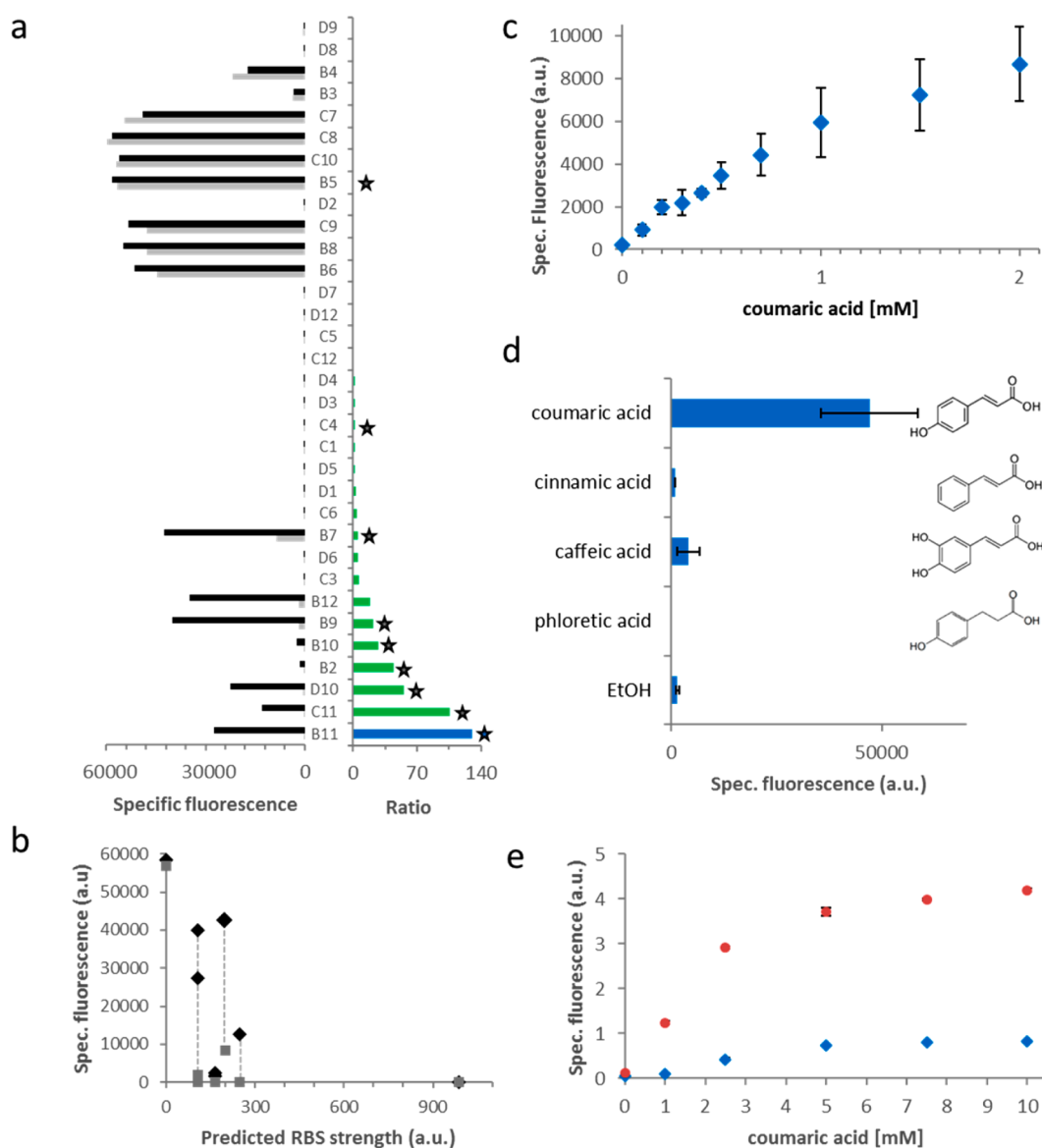


**Figure 3.** Identification and characterization of the *p*-coumaric acid biosensor. Results of the random mutagenesis of the RBS in front of PadR. (a) Specific fluorescence of XL1-blue cells harboring pG-PadR-RBS mutants cultured in the presence (black bars) and absence (gray bars) of 1 mM *p*-coumaric acid. The induction ratios with and without inducer are shown in green, and the best version is highlighted in blue and used for further experiments. Nine biosensor variants, labeled with stars, were further analyzed and sequenced. (b) The predicted RBS strengths of the selected clones were plotted against the specific fluorescence in the presence (black diamonds) and absence (gray diamonds) of *p*-coumaric acid. (c) The dynamic range of the biosensor. The specific fluorescence of EcPadR was determined following overnight cultivation in media supplemented with a range of *p*-coumaric acid concentrations. (d) Effector specificity of the biosensor. The specific fluorescence of EcPadR was determined following overnight cultivation in media supplemented with 1 mM of a number of chemicals structurally similar to *p*-coumaric acid. (e) The maximal specific fluorescence of *C. glutamicum* wild-type (blue diamonds) and *C. glutamicum*  $\Delta phdA$  (red circles) cells grown in the presence of different *p*-coumaric acid concentrations in a BioLector device. The specific fluorescence was determined as fluorescence per side scatter.

production strain, and the presented strategy of fine-tuning the expression strength of a repressor for optimal reversible repression will help in constructing additional biosensors for use in both *E. coli* and *C. glutamicum*.

**Sorting Yeast Producers with the Help of *E. coli* Biosensor Cells.** Biosensor-based screening represents a promising approach for the identification of importers,<sup>34</sup> but one of the major drawbacks in biosensor applications is that they are limited to measuring intracellular concentrations of small molecules. This limitation can be problematic, especially if intracellular product concentrations are kept low to reduce feedback regulation or toxicity due to the overexpression of

exporters.<sup>11</sup> In addition, secretion of the product into the extracellular space is generally preferred from a bioprocess perspective. To overcome this limitation, a sensor cell can be cocultivated with a production strain in microfluidic droplets. A requirement for measuring the efficiency of a producing cell by a nonproducing sensor cell in microdroplets is that the substrate and product are membrane permeable. To use biosensors to accurately detect a metabolite in a droplet, it is critical that the metabolite remain in the water droplet for long enough to affect the sensor and that it does not vanish into the surrounding fluorinated oil. To verify that *p*-coumaric acid does not partition into the oil and can activate the biosensor in

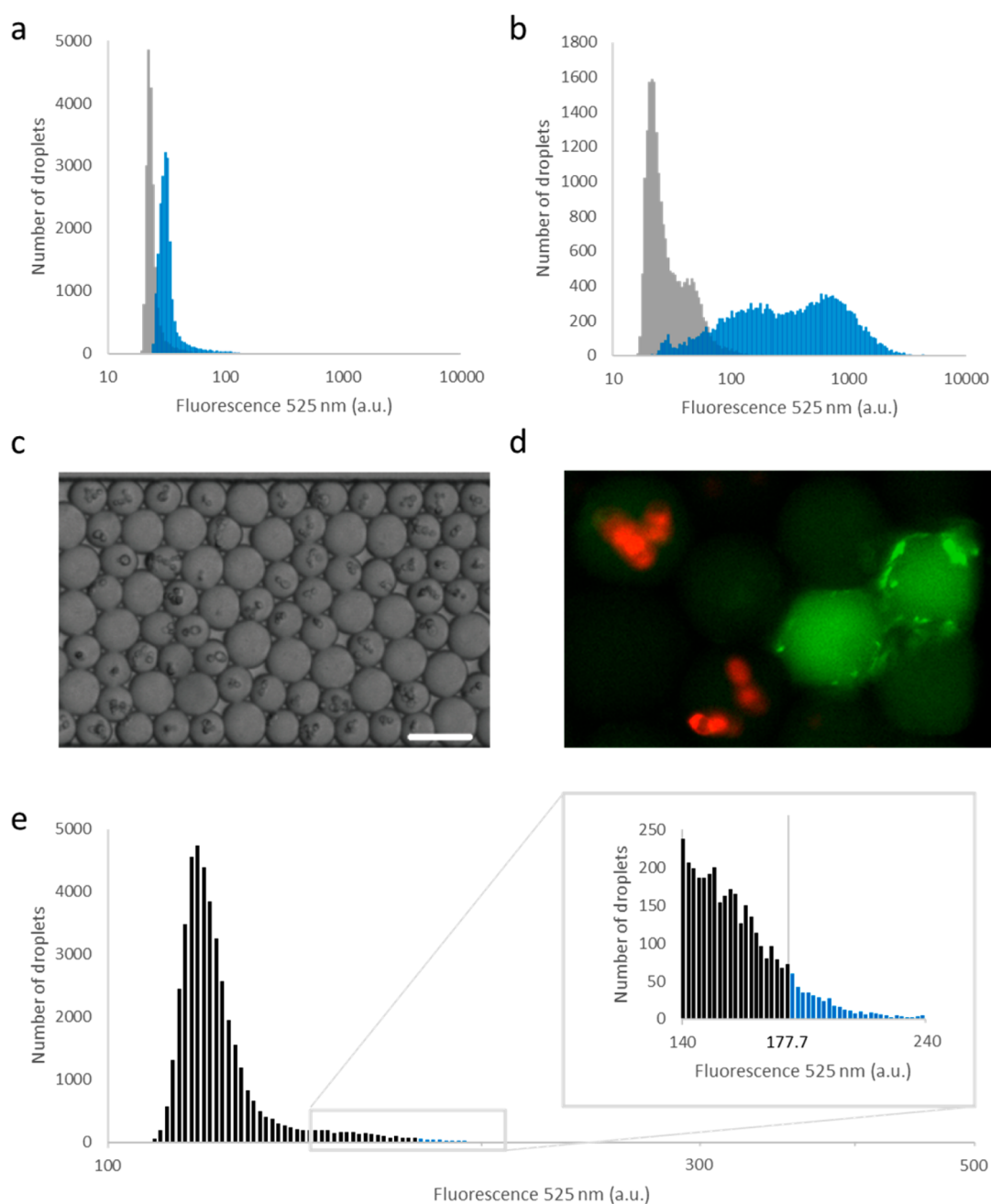


**Figure 4.** Detection and sorting according to biosensor cell response in picoliter droplets. (a,b) Histogram of droplet fluorescence at 525 nm from 20 000 individually measured droplets containing biosensor cells in the presence of 1 mM *p*-coumaric acid inducer (blue) or without *p*-coumaric acid (gray) measured (a) immediately following encapsulation and (b) after 7 h of incubation in the droplets. (c) A microscope image (scale bars, 50  $\mu$ m) shows that after 16 h of incubation of the mixture of yeast and *E. coli* cells in droplets, approximately one-fourth of the droplets (no yeast cells) increased in size, while the others decreased. (d) An overlay of fluorescence images shows that droplets containing RFP-expressing yeast do not emit yellow fluorescence. (e) A histogram of the droplet fluorescence of the model library upon sorting. The inset provides a magnified view of the sorting threshold level (solid line) and the sorted fraction of droplets (blue). The model library is composed of droplets containing *E. coli* biosensor cells coencapsulated with RFP-expressing yeast in 90% of the droplets and *p*-coumaric acid-producing yeast in 10% of the droplets.

microfluidic droplets, we grew the strain EcPadR in the presence of 1 mM *p*-coumaric acid in picoliter droplets generated at a rate of 1200 droplets per second in a microfluidic device. We injected *E. coli* at a concentration of  $6.84 \times 10^8$  cells/mL, corresponding to an average of 10 cells per droplet. The fluorescence of individual droplets was measured at the onset of induction immediately following droplet encapsulation (Figure 4a) as well as after 7 h of incubation in the droplets (Figure 4b). After 7 h, we detected significant increases in

fluorescence in nearly all droplets containing *p*-coumaric acid. The vast majority of droplets containing *p*-coumaric acid (83%) could be distinguished from droplets that did not contain *p*-coumaric acid based on the *E. coli* biosensor signal by applying a threshold that allows for a 2% false-positive rate (Figure 4b). This finding indicates that sorting for droplets containing *p*-coumaric acid based on a biosensor signal should be possible. Because YFP requires oxygen to mature and become fluorescent,<sup>35</sup> we needed to determine that sufficient oxygen

was available in the droplets. Additional oxygen can be supplied to the droplets by exchanging the fluorinated oil that the droplets are incubated in because the oil dissolves considerable amounts of oxygen. Exchanging the oil used during incubation led to an increase in fluorescence compared to droplets for which the oil was not exchanged (Supplementary Figure 2).

Further, we wanted to determine whether screening and sorting droplet-encapsulated producer cells would be possible based on the fluorescence signal generated by coencapsulated sensor cells (Figure 1).

Yeast has been shown to be an excellent *p*-coumaric acid producer,<sup>23,25</sup> but most of the genetic devices responsive to small molecules are derived from bacteria. In recent years, several novel strategies have been developed that utilize bacterial transcription factors in yeast for screening and pathway control.<sup>36–39</sup> Here, we demonstrate an alternative approach independent of intracellular concentration in the yeast producer cell.

We encapsulated two populations of yeast cells individually in microdroplets, generated at a rate of 5900 droplets per second, one *p*-coumaric acid-producing yeast strain (ST4058)<sup>25</sup> and another nonproducing yeast strain. The yeast strain that did not produce *p*-coumaric acid expressed RFP, which allowed us to distinguish between the two yeast strains after sorting. *p*-Coumaric was produced *de novo* from glucose or L-tyrosine present in the cultivation media (Supplemental Figure 3). The two droplet populations were mixed with a ratio of 10% producer cells and 90% nonproducing yeast cells. EcPadR *E. coli* biosensor cells were coencapsulated with yeast cells in all microdroplets. The droplets contained an average of 1.4 yeast cells and 7.7 *E. coli* sensor cells; 75% of the droplets therefore contained at least one yeast cell according to a Poisson distribution model. After generation, the droplets were stored at 30 °C in a collection syringe.

After 16 h of incubation, 74% of the droplets had decreased in size, whereas the remaining 26% had grown larger (Figure 4c). The quarter of the droplets that had increased in size contained no yeast cells, except in rare cases (<1%) in which the yeast cell was assumed to be dead. The larger droplets and smaller droplet populations had mean diameters of  $35.1 \pm 0.23 \mu\text{m}$  and  $27.1 \pm 0.32 \mu\text{m}$  (mean  $\pm$  SEM,  $n = 25$  in both cases), respectively. Size differences due to osmosis between droplets containing yeast following incubation was previously observed<sup>40</sup> and has been shown to be caused by water transport between droplets<sup>41</sup> driven by differences in solute concentrations generated as the yeast in the yeast-containing droplets consume sugars from the media (Figure 4c). No significant size differences were detected between different cell-containing droplets.

After the 16-h incubation period, the *E. coli* sensor emitted a detectable YFP fluorescence signal (shown in green in Figure 4d) in droplets containing non-RFP yeast cells (*p*-coumaric acid producers) but not in droplets containing RFP-expressing yeast cells or in those not containing any yeast cells, when exposed to laser light. This difference demonstrates that reporter genes are only expressed at detectable levels in *E. coli* sensor cells coencapsulated with *p*-coumaric acid-producing yeast cells and that *p*-coumaric acid is not transported between droplets on the time scale of the experiment. After 16 h of incubation, the top 1% of droplets were sorted in a microfluidic device based on the EcPadR YFP signal (Figure 4e). Sorting was performed at a rate of 300 droplets per second. The sorted yeast cells were incubated on agar plates and analyzed

individually for RFP fluorescence (indicating a nonproducing cell) by fluorescence microscopy (Table 1), and the RFP

**Table 1. Strain Verification after Sorting<sup>a</sup>**

method	<i>p</i> -CA clones %		enrichment factor	
	expt no. 1	expt no. 2	expt no. 1	expt no. 2
fluorescent microscopy	76.4	80.7	29	38
microtiter plate culture	77	87.5	30	63

<sup>a</sup>The sorted clones from a starting droplet population with 10% *p*-CA producers and 90% nonproducers were grown on agar plates and characterized by either fluorescence microscopy or culturing in microtiter plates followed by RFP fluorescence measurement. The table shows the percentage of *p*-coumaric acid (*p*-CA)-producing clones as well as the enrichment factor.

fluorescence of individual overnight cultures was measured (Table 1). We observed that between 76.4% and 87.5% of clones produced *p*-coumaric acid, achieving an enrichment factor of at least 30 (calculated by a cellular enrichment model 15) following a single round of sorting (Table 1). This finding demonstrates that microfluidic picoliter droplet sorting based on fluorescence from a coencapsulated sensor cell can be applied to identify a producer strain.

**Sorting of Yeast Producer Strain Library.** We further wanted to validate our method by analyzing the sorting capacity for a small library of production strains. In particular, we wanted to assess (i) the stability of the producer strains during the sorting process, (ii) the enrichment of producer cells after one and two rounds of sorting, and (iii) the ability to differentiate between high and low producers.

We decided to analyze a small library comprising 28 yeast strains, that had been shown to produce different amounts of *p*-coumaric acid.<sup>25</sup> In this experiment, we encapsulated one yeast strain per droplet together with *E. coli* biosensor cells and sorted them based on the biosensor signal. The droplets with the highest fluorescence (top 1%) were sorted in a first round and used as a template for a second round of sorting where again the droplets with the highest fluorescent signal (top 1%) were isolated.

After sorting, the yeast cells were grown in YPD media and the yield of *p*-coumaric acid was analyzed after 48 h. In total, 68 strains from the library, 8 strains after the first round and 24 after the second round of sorting were analyzed (Figure 5a,b). As expected, the library showed 15% producing cells with very different productivities, ranging from 0.03–0.68 mM *p*-coumaric acid. After a single round of sorting, already 50% of the eight tested cells produced *p*-coumaric acid. Three out of the four producing strains showed a similar or even higher *p*-coumaric acid yield after 48 h compared to the best strain of the analyzed strains from the library (0.17, 0.55, 0.66, and 0.96 mM *p*-coumaric acid). After the second round of sorting, 23 out of the 24 yeast strains produced *p*-coumaric acid (96%) with a very similar yield of  $0.17 \pm 0.05 \text{ mM}$  *p*-coumaric acid excluding one outlier (0.9 mM) (Figure 5b). These results show, that two rounds of sorting enables the enrichment of producing strains.

To apply our method to other biosensors and different production strains, the limitations and advantages of this method need to be taken into consideration. A single round of sorting results in a moderate enrichment of producing cells, hence multiple rounds of sorting are needed to screen complex and diverse cell libraries. Also, the incubation time between

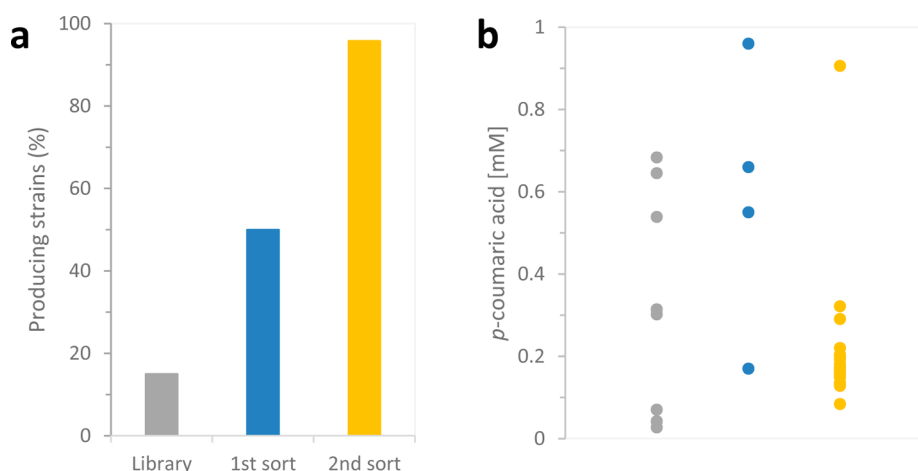


**Figure 5.** Enrichment of *p*-coumaric acid producers in a library screening. Library (gray) and the yeast cells isolated in the first (blue) and second (orange) round of sorting were grown in YPD media, and the yield of *p*-coumaric acid was analyzed after 48 h by HPLC: (a) percentage of producing cells; (b) individual *p*-coumaric acid yield of the analyzed strains.

sorting rounds needs to be reduced to a minimum to reduce fitness related reduction in high-performing producer cells.

The microfluidic format does impose specific limitations in terms of sensitivity and precision. For instance, fluorescence measurements on microtiter plates are generally repeated several times per well and averaged, whereas in droplet microfluidics each droplet is only measured a single time in a sorting experiment with short exposure times. Moreover, assaying single cells or microclones rather than larger populations decreases accuracy due to single cell variability. These effects are similar to other high throughput single cell techniques such as flow cytometry and can be overcome with multiple rounds of enrichment sorting.

Overall, droplet microfluidics provides an alternative to robotic microtiter plate and gel-encased bead sorting methods for cell factory library screening for extracellular products.<sup>19</sup> Both of the latter methods have been demonstrated to be effective but are limited in throughput to 1–10 wells or vessels per second and require longer incubation times due to the large volume of each isolated producer cell.

The inclusion of a cell biosensor in the droplets should greatly expand the range of target products available for droplet-based screening. Previously, droplet screens for extracellular products have been limited to secreted enzymes with available fluorogenic substrates and to products detectable by enzyme-linked assays with a fluorescent readout. Co-encapsulation in picoliter droplets allows separating the production and sensing functions previously harbored by a single cell. This separation allows optimization of each cell according to its function without the addition of an unnecessary metabolic load. Biosensor cells can be optimized for specificity and detection range and can be reused without the need for additional genetic manipulations. Likewise, selected producer strains can be transferred directly to scaled-up production testing in larger volumes. Many new biosensors will become available as the principles of biosensor engineering are better understood to meet the increasing need for metabolite biosensors. Our approach has a broad range of applications for screening extracellular chemical production using a novel bacterial biosensor.

## METHODS

### Microbial Strains, Media, and Growth Conditions.

Bacterial and yeast strains, as well as plasmids, are listed in [Supplementary Table 1](#). *E. coli* strains were transformed as previously described by Hanahan<sup>42</sup> and cultivated in LB medium,<sup>43</sup> 2xYT medium (16 g L<sup>-1</sup> tryptone, 10 g L<sup>-1</sup> yeast extract, 5 g L<sup>-1</sup> sodium chloride) or M9 minimal medium<sup>44</sup> containing 10 g L<sup>-1</sup> glucose. Yeast cells were cultivated in YPD medium (20 g L<sup>-1</sup> bacterial peptone, 10 g L<sup>-1</sup> yeast extract, 20 g L<sup>-1</sup> glucose). *C. glutamicum* strains were transformed as previously described<sup>45</sup> and cultivated in CGXII minimal medium<sup>46</sup> with 2% (w/v) glucose. Forty-eight-well Flowerplates (m2p-laboratories GmbH, Baesweiler, Germany) with 750  $\mu$ L medium were inoculated from a preculture to an OD<sub>600</sub> of 1 and cultivated at 30 °C, 1200 rpm, a humidity of 85% and a throw of  $\phi$  3 mm in a BioLector device (m2p-laboratories GmbH, Baesweiler, Germany) capable of online monitoring of growth and fluorescence. The formation of biomass was monitored by measuring the backscattered light intensity at a wavelength of 620 nm (signal gain factor 10). YFP fluorescence was measured at an excitation wavelength of 508 nm and an emission wavelength of 532 nm (signal gain factor 20).

**Recombinant DNA work.** The primers used in this work are listed in [Supplementary Table 1](#). The plasmid pG-PadR-43 was ordered from Genart (Regensburg, Germany) and contained the native promoter with an RBS variant and open reading frame of PadR as well as the native promoter region of PadC. The native PadC gene was replaced by a yellow fluorescent protein (YFP). For construction of the plasmid pG-PadR-3665, the plasmid pG-PadR-43 was used as a template in a site-directed mutagenesis PCR carried out using the primer pair padR-sdm\_for/padR-sdm\_rev. The PCR product was digested with DpnI, column purified using NucleoSpin Gel and a PCR Clean-Up kit (Macherey-Nagel, Düren, Germany), and transformed into XI-1-Blue cells. Random mutagenesis was carried out in a similar manner by taking pG-PadR-43 as the template and amplifying with either the primer pair padR-X1\_for/padR-X2\_rev or padR-X3\_for/padR-X4\_rev to generate a PadR RBS mutant library. The PadR-YFP construct containing the best RBS (pG-PadR-B11 or PG-PadR-B10) was amplified with the primer pair PadR\_EcoRI\_for/PadR\_PstI\_r-ev and was cloned into pSEVA421 using the *EcoRI* and *PstI*

restriction sites to generate the pSEVA421-B11 and pSEVA421-B10 sensor plasmid. The sensor cassette of pSEVA421-B10 was amplified using the primer pair *PstI*\_SCpadR\_F/*PstI*\_SCpadR\_R, digested with the restriction endonuclease *PstI*, and ligated into the vector pCLTON2.

**Determination of Fluorescence.** Fluorescence and OD600 were determined using a SynergyMx plate reader (Biotek, United States). YFP fluorescence was measured at an excitation of 505 nm and emission of 545 nm, with the gain set to 90 if not otherwise stated. The specific fluorescence was defined as the fluorescence per OD600 value (given in a.u.). RFP fluorescence was measured at an excitation of 555 nm and emission of 584 nm.

**Droplet Generation.** A loop of *E. coli* sensor cells was inoculated into 10 mL of 2XYT culture media with appropriate antibiotics in 50 mL glass shake flasks. The flasks were shaken at 150 rpm in an incubator maintained at 37 °C. Similarly, yeast cultures (*p*-coumaric acid producers and cells expressing RFP) were grown at 30 °C in YPD medium. The culture was removed and washed with fresh medium, and the cell density was adjusted according to the cell-to-drop ratio. *p*-Coumaric acid at a final concentration of 1 mM was added to the sensor cells for induction as required.

Polydimethylsiloxane base (PDMS) fabricated chips were used to make surfactant-stabilized monodisperse water droplets in an oil phase. The oil used was HFE-7500 (3M, United States) with 1% EA surfactant (RainDance Technologies Inc., Billerica, MA, USA). To generate *E. coli* sensor droplets, the oil flow was 500  $\mu\text{L}/\text{h}$  and the aqueous flow rate was 100  $\mu\text{L}/\text{h}$ . For generating yeast and sensor cells in the same droplet, the oil flow rate was 2000  $\mu\text{L}/\text{h}$ , and the aqueous flow rate was 200  $\mu\text{L}/\text{h}$  for the yeast culture and 200  $\mu\text{L}/\text{h}$  for the *E. coli* sensor culture. The generated droplets were stored in a plastic syringe. In yeast-*E. coli* sensor droplets, droplets containing *p*-coumaric acid-producing yeast were generated over 5 min, followed by RFP yeasts over 45 min. The final droplet population therefore consisted of 90% nonproducing yeast (RFP) droplets and 10% *p*-coumaric acid-producing yeast droplets. The droplet emulsion was incubated at 30 °C for yeast-*E. coli* and at 37 °C for the *E. coli* sensor alone. During incubation, the cells grew and divided in the droplets and sensor cells detected the metabolite (*p*-coumaric acid) and produced reporter YFP. To enhance the oxygen available to the droplets, fluorinated oil was exchanged with fresh oil 1.5 h before taking fluorescence measurements. The fluorescence measurement was performed with a line laser as described in the sorting section below.

**Picoliter Droplet Sorting.** Droplets were injected into the sorting chip<sup>16</sup> at a flow rate of 20  $\mu\text{L}/\text{h}$  (300 droplets/s) and separated by oil (1% surfactant) at a flow rate of 500  $\mu\text{L}/\text{h}$ . A 491 nm laser beam (Cobolt Calypso CW < 100 mW, Sweden) was expanded in one dimension to form a line by a plano-concave lens and focused by a 40 $\times$  objective lens onto the channel close to the electrode in the microfluidic chip. YFP in the droplets were excited upon passing this point, and YFP fluorescence was detected using an emission filter (525/20 nm) and a photomultiplier tube (PMT, Hamatsu, Japan). The PMT was connected to a field-programmable gate array (National Instruments, United States) programmed to activate a voltage pulse when the detected fluorescence signal exceeded an intensity threshold set to include the brightest 1% of the droplets. The voltage pulse was then amplified in a high-voltage amplifier (TREK Inc., Lockport, NY, USA) connected to the built-in electrode. The main channel of the chip splits in two

downstream of the excitation/electrode point, where one channel leads to a waste container and the other leads to a collection port. The collection port was connected to a 1 mL plastic syringe with a withdrawal flow rate of 220  $\mu\text{L}/\text{h}$ . The amplified voltage pulse (0.6 kV, 500  $\mu\text{s}$ , 30 kHz) directed the droplet to the collection syringe, while in the absence of a pulse, droplets passed to the waste container. The experimental setup is schematically described in supplementary (Supplemental Figure 4)

**Incubation of Sorted Droplet Emulsion.** The sorted droplet emulsion was diluted 10-fold with YPD media, and 100  $\mu\text{L}$  of this mixture was distributed in YPD agar plates containing ampicillin (100  $\mu\text{g}/\text{mL}$ ) and kanamycin (50  $\mu\text{g}/\text{mL}$ ) resistance. This condition is necessary for yeast clones but not *E. coli* sensor cells to grow. The plates were incubated for 2 days at 30 °C.

**Strain Verification after Sorting.** The clones grown on agar plates were analyzed using two methods.

(A) Growth in microtiter plates and measurement of RFP fluorescence: A 96-well plate was filled with 200  $\mu\text{L}$  of synthetic medium per well. Single clones were picked from the agar plate and inoculated in a microtiter plate. For reference, half of the wells (48 wells) of a microtiter plate were loaded with RFP yeast culture, while half were loaded with *p*-coumaric acid-producing yeast culture. Both plates were incubated at 30 °C with shaking in a Spectramax M microtiter plate reader (Molecular Devices, Sunnyvale, CA, USA). After 16 h of incubation, fluorescence measurements were taken at an excitation of 550 nm and emission of 584 nm. A threshold between RFP-positive and RFP-negative colonies (*p*-coumaric acid producers) was set based on the reference culture.

(B) Colonies were transferred to a microscope slide and imaged using an inverted Nikon Eclipse Ti-E with objective lenses CFI Plan Fluor DL-10X/NA = 0.30 and CFI Super Plan Fluor ELWD ADM 40X/NA = 0.60 equipped with a Lumencor SOLA II Solid State White Light Engine at 50% power output, an Andor Zyla sCMOS 5.5 camera, and a Semrock filter set (excitation 554/23, DM 573, emission 609/54). A threshold between RFP-positive and RFP-negative colonies was determined by imaging the reference strains.

**Sorting of Producer Cells from a Small Library.** Overnight cultures of the *E. coli* sensor strain p421B11 (grown in LB with spectinomycin) and 28 independent cultures of *p*-coumaric acid producing or nonproducing yeast strains (Supplementary Table 1) (grown in YPD) were prepared as follows: the *E. coli* cells were rediluted in LB, grown for 2 h until the exponential phase and were then pelleted and rediluted in YPD to a final concentration OD<sub>600</sub> = 1.7. All yeast cultures were in the stationary phase and were pooled at equal volume, except for the high producer "4058" which was added at half volume and the nonproducing RFP-expressing strain which was added in excess. The final fractions are about 20% RFP nonproducer, 1.5% "4058", and 3% each of the other 26 strains. The pooled mini-library was pelleted, and washed and rediluted in YPD to approximately final OD<sub>600</sub> = 3. Droplet generation for coencapsulation was immediately performed as described above. The collected emulsion was incubated at 30 °C for 6 h and the oil-surfactant mix was then replaced with new oil-surfactant. Following an additional 2 h incubation at 30 °C, sorting was performed as described above with gating on the top 1% of the droplets. A part of the sorted material was spread on YPD agar plates and the rest was inoculated in fresh YPD media. Following overnight incubation,



the yeast culture was again washed and prepared and encapsulated with *E. coli* sensor cells. A second round of sorting was done in the same way as described.

The analysis of productivity of the isolated strains was performed as previously described with minor changes.<sup>25</sup> The isolated strains were inoculated at 30 °C in 0.5 mL of YPD media in a 96-deepwell plate with 250 rpm agitation at 5 cm orbit overnight. Fermentation was carried out for 48 h at the same conditions as above. Afterward, the cultivation broth was centrifuged, and the supernatant was analyzed for *p*-coumaric acid concentrations using HPLC.

## ■ ASSOCIATED CONTENT

### ● Supporting Information

The Supporting Information is available free of charge on the ACS Publications website at DOI: 10.1021/acssynbio.7b00009.

Tables: strains, plasmids and oligonucleotides used in this work; ribosome binding site sequences of selected mutants. Figures: time dependency of biosensor response; effect of oxygen availability on YFP fluorescence in picodroplets; production pathway of *p*-coumaric acid from glucose and tyrosine present in the cultivation medium; schematic drawing of the picoliter sorting setup (PDF)

## ■ AUTHOR INFORMATION

### Corresponding Author

\*E-mail: msom@bio.dtu.dk.

### ORCID

Solvej Siedler: 0000-0002-5445-8792

Narendar K. Khatri: 0000-0003-4101-855X

Jan Marienhagen: 0000-0001-5513-3730

Morten O. A. Sommer: 0000-0003-4005-5674

### Author Contributions

S.S. and H.N.J. conceived this project. S.S., N.K.K., A.Z., I.K., C.F.N., M.V., and P.H. performed all of the experiments. S.S., N.K.K., P.H., J.M., M.O.A.S., and H.N.J. analyzed the data. S.S., N.K.K., M.O.A.S., and H.N.J. wrote the manuscript.

### Notes

The authors declare no competing financial interest.

## ■ ACKNOWLEDGMENTS

We thank Irina Borodina from the Novo Nordisk Foundation Center for Biosustainability at the Technical University of Denmark for providing the yeast strains. This study was supported by the Novo Nordisk Foundation as “Biosensor-based genome screening platform for the production of Biosynthetic Precursors and coFactors in *E. coli*” under Grant Agreement No. 11335. Solvej Siedler’s and Morten Sommer’s research was funded by the European Union Seventh Framework Programme (FP7-KBBE-2013-7-single-stage) under Grant Agreement No. 613745, Promys.

## ■ REFERENCES

- (1) Jiang, W., Bikard, D., Cox, D., Zhang, F., and Marraffini, L. A. (2013) RNA-guided editing of bacterial genomes using CRISPR-Cas systems. *Nat. Biotechnol.* 31, 233–239.
- (2) Bonde, M. T., Kosuri, S., Genee, H. J., Sarup-Lytzen, K., Church, G. M., Sommer, M. O., and Wang, H. H. (2015) Direct Mutagenesis of Thousands of Genomic Targets Using Microarray-Derived Oligonucleotides. *ACS Synth. Biol.* 4, 17–22.
- (3) Kosuri, S., and Church, G. M. (2014) Large-scale de novo DNA synthesis: technologies and applications. *Nat. Methods* 11, 499–507.
- (4) Mahr, R., and Frunzke, J. (2016) Transcription factor-based biosensors in biotechnology: current state and future prospects. *Appl. Microbiol. Biotechnol.* 100, 79–90.
- (5) Eggeling, L., Bott, M., and Marienhagen, J. (2015) Novel screening methods—biosensors. *Curr. Opin. Biotechnol.* 35, 30–36.
- (6) Michener, J. K., and Smolke, C. D. (2012) High-throughput enzyme evolution in *Saccharomyces cerevisiae* using a synthetic RNA switch. *Metab. Eng.* 14, 306–316.
- (7) Siedler, S., Stahlhut, S. G., Malla, S., Maury, J., and Neves, A. R. (2014) Novel biosensors based on flavonoid-responsive transcriptional regulators introduced into *Escherichia coli*. *Metab. Eng.* 21, 2–8.
- (8) Binder, S., Siedler, S., Marienhagen, J., Bott, M., and Eggeling, L. (2013) Recombineering in *Corynebacterium glutamicum* combined with optical nanosensors: a general strategy for fast producer strain generation. *Nucleic Acids Res.* 41, 6360.
- (9) Raman, S., Rogers, J. K., Taylor, N. D., and Church, G. M. (2014) Evolution-guided optimization of biosynthetic pathways. *Proc. Natl. Acad. Sci. U. S. A.* 111, 17803–17808.
- (10) Siedler, S., Schendzielorz, G., Binder, S., Eggeling, L., Bringer, S., and Bott, M. (2014) SoxR as a Single-Cell Biosensor for NADPH-Consuming Enzymes in *Escherichia coli*. *ACS Synth. Biol.* 3, 41–47.
- (11) Binder, S., Schendzielorz, G., Stähler, N., Krumbach, K., Hoffmann, K., Bott, M., and Eggeling, L. (2012) A high-throughput approach to identify genomic variants of bacterial metabolite producers at the single-cell level. *Genome Biol.* 13, R40.
- (12) Wang, B. L., Ghaderi, A., Zhou, H., Agresti, J., Weitz, D. A., Fink, G. R., and Stephanopoulos, G. (2014) Microfluidic high-throughput culturing of single cells for selection based on extracellular metabolite production or consumption. *Nat. Biotechnol.* 32, 473–478.
- (13) Joensson, H. N., and Andersson Svahn, H. (2012) Droplet Microfluidics—A Tool for Single-Cell Analysis. *Angew. Chem., Int. Ed.* 51, 12176–12192.
- (14) Agresti, J. J., Antipov, E., Abate, A. R., Ahn, K., Rowat, A. C., Baret, J.-C., Marquez, M., Klibanov, A. M., Griffiths, A. D., and Weitz, D. A. (2010) Ultrahigh-throughput screening in drop-based microfluidics for directed evolution. *Proc. Natl. Acad. Sci. U. S. A.* 107, 4004–4009.
- (15) Baret, J.-C., Miller, O. J., Taly, V., Ryckelynck, M., El-Harrak, A., Frenz, L., Rick, C., Samuels, M. L., Hutchison, J. B., Agresti, J. J., Link, D. R., Weitz, D. A., and Griffiths, A. D. (2009) Fluorescence-activated droplet sorting (FADS): efficient microfluidic cell sorting based on enzymatic activity. *Lab Chip* 9, 1850–1858.
- (16) Sjöström, S. L., Bai, Y., Huang, M., Liu, Z., Nielsen, J., Joensson, H. N., and Andersson Svahn, H. (2014) High-throughput screening for industrial enzyme production hosts by droplet microfluidics. *Lab Chip* 14, 806–813.
- (17) Huang, M., Bai, Y., Sjöström, S. L., Hallström, B. M., Liu, Z., Petranovic, D., Uhlén, M., Joensson, H. N., Andersson-Svahn, H., and Nielsen, J. (2015) Microfluidic screening and whole-genome sequencing identifies mutations associated with improved protein secretion by yeast. *Proc. Natl. Acad. Sci. U. S. A.* 112, E4689–E4696.
- (18) Hammar, P., Angermayr, S. A., Sjöström, S. L., van der Meer, J., Hellingwerf, K. J., Hudson, E. P., and Joensson, H. N. (2015) Single-cell screening of photosynthetic growth and lactate production by cyanobacteria. *Biotechnol. Biofuels* 8, 492.
- (19) Meyer, A., Pellaux, R., Potot, S., Becker, K., Hohmann, H.-P., Panke, S., and Held, M. (2015) Optimization of a whole-cell biocatalyst by employing genetically encoded product sensors inside nanoliter reactors. *Nat. Chem.* 7, 673–678.
- (20) Marienhagen, J., and Bott, M. (2013) Metabolic engineering of microorganisms for the synthesis of plant natural products. *J. Biotechnol.* 163, 166–178.
- (21) Nguyen, T. K. C., Tran, N. P., and Cavin, J.-F. (2011) Genetic and Biochemical Analysis of PadR-padC Promoter Interactions during the Phenolic Acid Stress Response in *Bacillus subtilis* 168. *J. Bacteriol.* 193, 4180–4191.

- (22) Tran, N. P., Gury, J., Dartois, V., Nguyen, T. K. C., Seraut, H., Barthelmebs, L., Gervais, P., and Cavin, J.-F. (2008) Phenolic Acid-Mediated Regulation of the *padC* Gene, Encoding the Phenolic Acid Decarboxylase of *Bacillus subtilis*. *J. Bacteriol.* *190*, 3213–3224.
- (23) Jendresen, C. B., Stahlhut, S. G., Li, M., Gaspar, P., Siedler, S., Förster, J., Maury, J., Borodina, I., and Nielsen, A. T. (2015) Highly Active and Specific Tyrosine Ammonia-Lyases from Diverse Origins Enable Enhanced Production of Aromatic Compounds in Bacteria and *Saccharomyces cerevisiae*. *Appl. Environ. Microbiol.* *81*, 4458–4476.
- (24) van Summeren-Wesenhagen, P. V., Voges, R., Dennig, A., Sokolowsky, S., Noack, S., Schwaneberg, U., and Marienhagen, J. (2015) Combinatorial optimization of synthetic operons for the microbial production of *p*-coumaryl alcohol with *Escherichia coli*. *Microb. Cell Fact.* *14*, 498.
- (25) Rodriguez, A., Kildegaard, K. R., Li, M., Borodina, I., and Nielsen, J. (2015) Establishment of a yeast platform strain for production of *p*-coumaric acid through metabolic engineering of aromatic amino acid biosynthesis. *Metab. Eng.* *31*, 181–188.
- (26) Cashin, P., Goldsack, L., Hall, D., and O'Toole, R. (2006) Contrasting signal transduction mechanisms in bacterial and eukaryotic gene transcription. *FEMS Microbiol. Lett.* *261*, 155–164.
- (27) Rugbjerg, P., Genee, H. J., Jensen, K., Sarup-Lytzen, K., and Sommer, M. O. A. (2016) Molecular Buffers Permit Sensitivity Tuning and Inversion of Riboswitch Signals. *ACS Synth. Biol.* *5*, 632.
- (28) Espah Borujeni, A., Channarasappa, A. S., and Salis, H. M. (2014) Translation rate is controlled by coupled trade-offs between site accessibility, selective RNA unfolding and sliding at upstream standby sites. *Nucleic Acids Res.* *42*, 2646–2659.
- (29) Bonde, M. T., Pedersen, M., Klausen, M. S., Jensen, S. I., Wulff, T., Harrison, S., Nielsen, A. T., Herrgård, M. J., and Sommer, M. O. A. (2016) Predictable tuning of protein expression in bacteria. *Nat. Methods* *13*, 233.
- (30) Kües, U., and Stahl, U. (1989) Replication of plasmids in gram-negative bacteria. *Microbiol. Rev.* *53*, 491–516.
- (31) Hirakawa, H., Schaefer, A. L., Greenberg, E. P., and Harwood, C. S. (2012) Anaerobic *p*-Coumarate Degradation by *Rhodospseudomonas palustris* and Identification of CouR, a MarR Repressor Protein That Binds *p*-Coumaroyl Coenzyme A. *J. Bacteriol.* *194*, 1960–1967.
- (32) Parke, D., and Ornston, L. N. (2003) Hydroxycinnamate (*hca*) Catabolic Genes from *Acinetobacter* sp. Strain ADP1 Are Repressed by HcaR and Are Induced by Hydroxycinnamoyl-Coenzyme A Thioesters. *Appl. Environ. Microbiol.* *69*, 5398–5409.
- (33) Kallscheuer, N., Vogt, M., Kappelmann, J., Krumbach, K., Noack, S., Bott, M., and Marienhagen, J. (2016) Identification of the *phd* gene cluster responsible for phenylpropanoid utilization in *Corynebacterium glutamicum*. *Appl. Microbiol. Biotechnol.* *100*, 1871–1881.
- (34) Genee, H. J., Bali, A. P., Petersen, S. D., Siedler, S., Bonde, M. T., Gronenberg, L. S., Kristensen, M., Harrison, S. J., and Sommer, M. O. A. (2016) Functional mining of transporters using synthetic selections. *Nat. Chem. Biol.* *12*, 1015–1022.
- (35) Heim, R., Prasher, D., and Tsien, R. (1994) Wavelength mutations and posttranslational autoxidation of green fluorescent protein. *Proc. Natl. Acad. Sci. U. S. A.* *91*, 12501–12504.
- (36) David, F., Nielsen, J., and Siewers, V. (2016) Flux Control at the Malonyl-CoA Node through Hierarchical Dynamic Pathway Regulation in *Saccharomyces cerevisiae*. *ACS Synth. Biol.* *5*, 224–233.
- (37) Teo, W. S., and Chang, M. W. (2015) Bacterial XylRs and synthetic promoters function as genetically encoded xylose biosensors in *Saccharomyces cerevisiae*. *Biotechnol. J.* *10*, 315–322.
- (38) McIsaac, R. S., Gibney, P. A., Chandran, S. S., Benjamin, K. R., and Botstein, D. (2014) Synthetic biology tools for programming gene expression without nutritional perturbations in *Saccharomyces cerevisiae*. *Nucleic Acids Res.* *42*, e48.
- (39) Skjoedt, M. L., Snoek, T., Kildegaard, K. R., Arsovska, D., Eichenberger, M., Goedecke, T. J., Rajkumar, A. S., Zhang, J., Kristensen, M., Lehka, B. J., Siedler, S., Borodina, I., Jensen, M. K., and Keasling, J. D. (2016) Engineering prokaryotic transcriptional activators as metabolite biosensors in yeast. *Nat. Chem. Biol.* *12*, 951–958.
- (40) Joensson, H. N., Uhlén, M., and Svahn, H. A. (2011) Droplet size based separation by deterministic lateral displacement—separating droplets by cell-induced shrinking. *Lab Chip* *11*, 1305.
- (41) Hofmann, T. W., Hänselmann, S., Janiesch, J.-W., Rademacher, A., and Böhm, C. H. J. (2012) Applying microdroplets as sensors for label-free detection of chemical reactions. *Lab Chip* *12*, 916.
- (42) Hanahan, D. (1983) Studies on transformation of *Escherichia coli* with plasmids. *J. Mol. Biol.* *166*, 557–580.
- (43) Miller, J. H. (1972) *Experiments in Molecular Genetics*, Cold Spring Harbor Laboratory, Cold Spring Harbor, N.Y.
- (44) Sambrook, J., and Russel, D. W. (2001) *Molecular Cloning. A Laboratory Manual*, 3rd ed., Cold Spring Harbor Laboratory Press, Cold Spring Harbor, NY.
- (45) Eggeling, L., and Bott, M. (2005) *Handbook of Corynebacterium Glutamicum*, Taylor & Francis, Boca Raton.
- (46) Keilhauer, C., Eggeling, L., and Sahm, H. (1993) Isoleucine synthesis in *Corynebacterium glutamicum*: molecular analysis of the *ilvB-ilvN-ilvC* operon. *J. Bacteriol.* *175*, 5595–5603.